Marine Mammal Science

Marine Mammal Science

ARTICLE

Elevating Photo-Identification: Aerial-Identification Improves Re-Sight Rates and Supports Long-Term Monitoring of Humpback Whales

Lewis I. Evans[1,2] | Martin van Aswegen[1,2] | Sonja Feinberg[1] | Jens J. Currie[1,3] | Stephanie H. Stack[4] | Andrew Szabo[1,2] | Lars Bejder[1]

[1]Marine Mammal Research Program, Hawai'i Institute of Marine Biology, University of Hawai'i at Mānoa, Kāne'ohe, Hawai'i, USA | [2]Alaska Whale Foundation, Petersburg, Alaska, USA | [3]Pacific Whale Foundation, Mā'alaea, Hawai'i, USA | [4]Southern Ocean Persistent Organic Pollutants Program, School of Environment and Science, Griffith University, Brisbane, Queensland, Australia

Correspondence: Lewis I. Evans (levans4@hawaii.edu)

Received: 4 June 2025 | **Revised:** 9 September 2025 | **Accepted:** 14 September 2025

Funding: Hawai'i fieldwork was made possible through the University of Hawai'i at Mānoa, DoD's Defense University Research Instrumentation Program (Award No. N00014-19-2612 and N00014-21-1-2249), Office of Naval Research (Award No. N000142012624), 'Our Oceans' Netflix, Wildspace Productions and Freeborne Media, Omidyar Ohana Foundation, and PacWhale Eco-Adventures as well as members and donors of Pacific Whale Foundation. Southeast Alaska research was funded through awards from the National Geographic Society (NGS), Lindblad Expeditions-National Geographic (LEX-NG) Funds and North Pacific Research Board (#2114).

Keywords: body condition | cookiecutter shark | drone | individual monitoring | photo-identification | tubercle

ABSTRACT

Photo-identification (photo-ID) is a widely used, non-invasive method for monitoring individual animals, including humpback whales (*Megaptera novaeangliae*; HBWs), and has provided valuable insights into their population dynamics, movement patterns, and social structures. Traditional identification relies on the trailing edge and ventral pigment patterns of the tail fluke (fluke-ID); however, not all whales present their flukes, limiting identification and re-sighting opportunities. We developed a novel aerial-identification (aerial-ID) approach using drone imagery to identify individual HBWs based on the arrangement of two features, tubercles (TB) and cookiecutter shark scars (CCS). Between January and March 2022, we sampled 1498 HBWs, including repeated individuals, capturing fluke-ID images for 772 and aerial-ID images for 1437. Fluke-ID yielded 164 re-sightings (76 lactating females, 88 others), while aerial-ID yielded 372 (249 and 123, respectively), representing a 227% increase for lactating females and 40% for others. We extended this approach to a multi-year, cross-regional dataset (2018–2025) of 54 individuals verified with fluke-ID. All were matched using aerial-ID, with the longest re-sight spanning 2737 days (6.5 years), representing the maximum interval within our study period. Aerial-ID thus offers a powerful complement to fluke-ID, expanding demographic coverage, increasing re-sighting rates, and enabling long-term, cross-regional monitoring.

HŌ'ULU'ULU

He 'ano hana laha a ho'oluhi 'ole ka hō'oia ki'i no ke kilo 'ana i nā holoholona, e like me ke koholā (*Megaptera novaeangliae*), a hō'ike nō i ko lākou 'ano lehulehu, kā lakou holo 'ana, me nā pilina 'ohana. Kauka'i ka hō'oia laha i ke 'ano o ke ka'e o ka hi'u a me ka waiho'olu'u i lalo o ka hi'u (hō'oia hi'u); akā na'e, 'a'ole 'ike 'ia ka hi'u o nā koholā a pau, e ho'ēmi ana i nā hō'oia a me nā 'ike hou. Ua ho'okumu 'ia kekahi 'ano hana hō'oia lani e mākou e ho'ohana ana i ka pa'i ki'i 'ana o ka helekopa uila li'i i mea e hō'oia ai i nā koholā ma o ke 'ano o 'elua mea, nā pu'u a me nā 'ālina manō cookiecutter. Ma waena o 'Ianuali me Malaki 2022, 'ike 'ia 1498 mau koholā, me nā 'ike hou, a pa'i ki'i 'ia 772 ki'i hō'oia hi'u me 1437 ki'i hō'oia lani. Ua loa'a 164 'ike hou (76 wāhine

e hānai ana, 88 koholoā ʻē aʻe) mai ka hōʻoia hiʻu, a loaʻa 372 (249 a me 123) mai ka hōʻoia lani, he hoʻonui 227% no nā wāhine e hānai ana a 40% no nā koholā ʻē aʻe. Hoʻohana nō hoʻi mākou i kēia ʻano hana ma kekahi papa ʻike o 54 mau koholā i hōʻoia ʻia e ka hōʻoia hiʻu mai 2018–2025 he nui nā wahi. Hoʻohālikelike ʻia nā koholā a pau e ka hōʻoia lani, a 2737 lā (6.5 makahiki) ka wā ʻike hou lōʻihi loa, ka wā nui loa ma kā mākou noiʻi. He hui maikaʻi nō ka hōʻoia lani me ka hōʻoia hiʻu, e hoʻonui ana i ka ʻike ʻana o nā ʻano koholā ʻokoʻa a me ka ʻike hou ʻana o kekahi koholā. No laila, ʻoi aku ke kilo ʻana no ka wā lōʻihi aʻe a me nā wahi ʻē.

1 | Introduction

Accurate identification of individual animals is foundational to wildlife research and conservation, with techniques ranging from genetic and AI-based approaches to traditional visual methods (Blount et al. 2022; Cheeseman et al. 2022; Taberlet and Luikart 1999; Wang 2016). Among these, photo-identification (photo-ID) has become a cornerstone in studies of long-lived, mobile species, particularly in marine megafauna, due to its non-invasive nature and effectiveness for tracking individuals over time (Bogucki et al. 2019; Brooks et al. 2010; Cheeseman et al. 2022). This method provides critical information on abundance (Hammond et al. 2021), demographic parameters (Borchers et al. 2014), movement patterns (McPherson et al. 2024), and social structures (Bejder et al. 1998). Such insights are instrumental in assessing population health and informing evidence-based management and conservation strategies (Taylor and Gerrodette 1993; Wilson et al. 1999).

In cetacean research, at least 57 species have been studied using photo-ID (Bichell et al. 2018) by identifying unique, stable natural markings, typically documented through photographic imagery of features such as dorsal fins (Würsig and Jefferson 1990) and tail flukes (Cheeseman et al. 2022; Katona et al. 1979; Katona and Whitehead 1981). Among these species are humpback whales (*Megaptera novaeangliae*; HBWs; Katona et al. 1979), which are identified by the relatively stable trailing edge shape, pigment patterns, and scarring on their ventral flukes (Katona et al. 1979; Schevill and Backus 1960). Photo-ID has provided decades of wide-scale monitoring and essential life history data on HBWs, supporting studies of population structure, abundance, and demographics (Cheeseman et al. 2024; Clapham et al. 1993; Fleming and Jackson 2011; Gabriele et al. 2017; Stevick et al. 2003; Zerbini et al. 2010). When integrated with advanced mark-recapture models, photo-ID serves as a pivotal tool for assessing population trajectories in response to previous and ongoing stressors, including the cessation of commercial whaling, climate change, vessel collisions, and entanglements (Calambokidis et al. 2008; Cheeseman et al. 2024; Fleming and Jackson 2011).

Global open-access platforms, such as Happywhale (https://happywhale.com/home), employ algorithm-assisted matching, which has enabled the identification of over 360,000 humpback whales through citizen science and large-scale research collaborations (Cheeseman et al. 2022, 2024). While photo-ID has enabled large-scale assessments of abundance, movement, and reproductive patterns, it relies on capturing high-quality photographs of the ventral surface of the tail.

Capturing photo-ID images of HBW tail flukes (hereafter referred to as "fluke-ID") can be challenging due to environmental conditions, such as glare, sea state, and swell, and variability in whale behavior, as individuals do not always "fluke-out", the act of raising their flukes above the water while diving. This is particularly problematic on breeding grounds, where whales may be less active or occupy shallow habitats that limit deep diving (Currie et al. 2018). While lactating females fluke-out in 93% of dives on Alaskan feeding grounds (A. Szabo, unpbl. data), fluking rates on the breeding grounds can be as low as 28% (Craig and Herman 1997; Rice et al. 1987). Lactating females invest considerable energetic resources during gestation and lactation (van Aswegen et al. 2025a; van Aswegen et al. 2025b); therefore, repeated identification of these individuals is crucial for understanding maternal expenditure and calf growth. More broadly, reduced reidentification opportunities hinder our ability to monitor individual whales across time, limiting resolution on physiological change, fine-scale habitat use, movement patterns, and reproductive behavior. As a result, there is a clear need for alternative or complementary identification methods that rely on other consistently visible features, such as dorsal fins (Patton et al. 2023) or lateral body pigment patterns (Kaufman et al. 1987).

Unoccupied aerial systems (UAS; i.e., drones) provide a non-invasive and cost-effective method to obtain high-resolution aerial imagery with minimal disturbance when operated at appropriate altitudes (Christiansen, Dujon, et al. 2016; Christiansen, Rojano-Doñate, et al. 2016; Christiansen, Nielsen, et al. 2020; Christiansen, Dawson, et al. 2020). The top-down perspective has facilitated the individual identification of multiple cetacean species, including bottlenose dolphins (*Tursiops truncatus*; Cheney et al. 2022), Risso's dolphins (*Grampus griseus*; Hartman et al. 2020), beluga whales (*Delphinapterus leucas*; Ryan et al. 2022), killer whales (*Orcinus orca*; Durban et al. 2015), bowhead whales (*Balaena mysticetus*; Koski et al. 2015), sperm whales (*Physeter macrocephalus*; O'Callaghan et al. 2024), and North Atlantic right whales (*Eubalaena glacialis*; Frasier et al. 2009). Automated pattern recognition software used on aerial images of North Atlantic right whale callosity patterns has proven effective in identifying individuals, enabling reliable monitoring across spatial and temporal scales (Bogucki et al. 2019). This aerial approach, known as aerial-identification (aerial-ID), has yielded critical insights into right whale population abundance, demographics, and bioenergetics, demonstrating its potential for other species (Bogucki et al. 2019; Christiansen, Nielsen, et al. 2020, Christiansen, Dawson, et al. 2020, Christiansen et al. 2023; Crowe et al. 2021; Stewart et al. 2021).

HBWs lack callosities, yet their dorsal surfaces exhibit distinctive features, such as tubercles (protruding sensory nodes, primarily located on the whale's head) and scarring (Best and Photopoulou 2016; Mercado 2014). These features, particularly tubercles, may be stable over time and, if consistently visible in aerial imagery, could support reliable identification across both short and long timescales. Such imagery is widely available in

UAS-based datasets for HBWs, often collected for photogrammetry, behavioral studies, or health assessments. The shared reliance of aerial-ID and these research applications on top-down imagery may allow both to be conducted in the same flight, reducing field effort and disturbance while expanding monitoring capacity. In contrast, fluke- and dorsal fin-ID require specific behaviors or viewing angles that are often unavailable, particularly in breeding ground contexts. Nonetheless, the application of aerial-ID remains largely unexplored, and most prior attempts have relied on visual assessments of body scarring or coloration from relatively small sample sizes (Bierlich et al. 2022; Martins et al. 2020; Napoli et al. 2024). Its effectiveness, particularly using pattern recognition software, has yet to be empirically tested.

Pattern recognition tools, such as the Interactive Individual Identification System (I^3S), have been successfully applied to species with stable distinguishing features, including mosquitoes and bees (Vyas-Patel and Mumford 2017), lizards (Sacchi et al. 2010), and sharks (Hook et al. 2019). While relatively simple and partially automated, I^3S offers a practical, accessible, free-to-use method for testing the feasibility of aerial-ID using top-down images.

Improved re-sighting of individuals is critical for characterizing abundance, habitat use, migratory timing, and physiological change, key metrics for assessing how populations respond to environmental and anthropogenic stressors. This study tests the hypothesis that aerial-ID can reliably distinguish individual HBWs and offer comparable or enhanced re-sighting potential relative to traditional fluke-ID. First, we assess whether aerial-ID increases individual and total re-sight rates within a single season. Building on this, we test identification matches across years and regions using tubercle patterns to demonstrate its utility for long-term individual identification. By applying this approach across a large dataset, this study provides the first quantitative assessment of aerial-ID for HBWs and demonstrates it as a valuable tool for improving short- and long-term individual monitoring.

2 | Materials and Methods

2.1 | Data Collection

We used UAS videography and vessel-based fluke photographs of HBWs collected for morphometric studies between 2018 and 2025. Data were obtained from two study regions (Figure 1): the Au'Au Channel, Maui Nui, Hawai'i (2018–2022, 2025) during the peak breeding season (January–March), and Southeast Alaska (2018–2020) during the feeding season

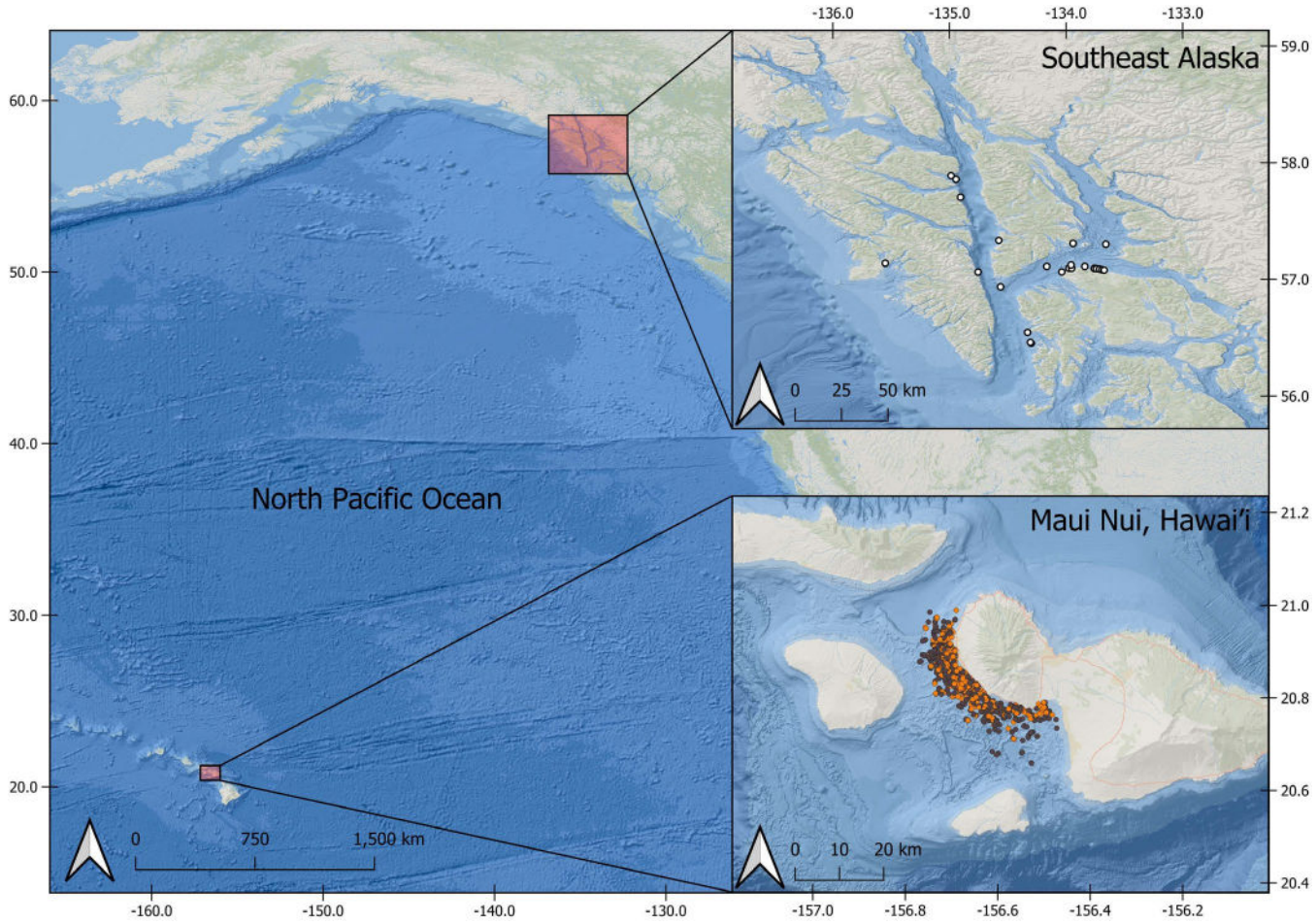

FIGURE 1 | Map showing the study areas across the North Pacific, including the feeding grounds of Southeast Alaska (top right) and the breeding grounds of Maui Nui, Hawai'i (bottom right). Locations of sampled lactating females within season are shown as orange points and others as black points. Locations of 'unclassified' individuals sampled multi-year and multi-regionally are shown as white points. The map was created using QGIS version 3.16.11-Hannover using ESRI Ocean Base Map (*Source:* https://plugins.qgis.org/plugins/quick_map_services/).

(June–September), a key foraging ground for the Hawai'i Distinct Population Segment.

For within-season analysis, we used concurrent aerial-ID and fluke-ID data collected in Maui Nui between January 5 and March 28, 2022 (Figure 1), representing the largest seasonal sample in our catalog. For multi-year and cross-regional analysis, we used aerial-ID images from 2019 to 2022 and 2025 in Maui Nui, and from 2018 to 2020 in Southeast Alaska, representing available matches across years and regions.

A small quadcopter (DJI Inspire 2, 3.3 kg, www.dji.com) equipped with one of two camera-lens systems was used to collect aerial IDs: a DJI Zenmuse X5s camera (Olympus 25 mm f1.8 rectilinear lens) or a DJI Zenmuse X7 camera (DJI 35 mm f2.8 LS ASPH rectilinear lens). We conducted UAS launches and retrievals from a small research vessel (< 28 ft) under favorable conditions (i.e., low wind, minimal swell, and no precipitation). While hovering over surfacing whales (altitude range = 25 to 55 m), high-resolution (3840 × 2160) videos were captured with the lens in nadir position.

We recorded the whale's location using a handheld Garmin GPS (73 Navigator) through vessel-based and aerial observations. Photo-identification images were taken of ventral flukes using a Nikon D500 camera and AF-S Nikkor 80–400 mm f4.5–5.6G ED VR lens. Images were taken to capture key identifiable features, including ventral fluke pigmentation, scarring, and trailing edge notches. All whales over which a UAS flight was conducted with the intent of collecting morphometric data were considered sampled individuals. Aerial-ID was attempted for each sampled whale, regardless of whether imagery ultimately met quality criteria for body condition assessment.

FIGURE 2 | The image depicts tubercles (orange circle) and cookiecutter shark scars (White circle) on top of the whale's head.

2.2 | Identifying Features From an Aerial Perspective

We identified individual HBWs from aerial imagery using the spatial arrangement of two primary features: Tubercles (TB) and cookiecutter shark (*Isistius* spp.) scars (CCS) (Figure 2). TBs are innervated sensory nodes on the dorso-lateral surfaces of the whale's head (Figure 2) and concentrated around the mouth, measuring approximately 10–15 cm in basal diameter (Mercado 2014; Tomilin 1967). These structures are densely packed with nerves and likely serve as tactile sensors, enabling the detection of changes in water pressure (Ling 1977), prey concentrations (Reeb et al. 2007), and low-frequency sounds (Yablokov et al. 1974). In this study, TBs were recognized by their protruding, nodular profile, often accompanied by shading and dark coloration or a reddish raw appearance due to abrasion from competitive behavior.

Cookiecutter scars are distinctive, circular bite marks caused by cookiecutter sharks, small ectoparasitic predators commonly found in pelagic tropical and subtropical habitats (Jahn and Haedrich 1988; Nakano and Nagasawa 1996; Figure 2). These scars appear on various marine megafauna, including elasmobranchs (Hoyos-Padilla et al. 2013), pelagic fishes (Niella et al. 2018), pinnipeds (Moreira-Mendieta et al. 2024), and cetaceans (Best and Photopoulou 2016; Walker-Milne et al. 2025). Our study classified CCS as indented, pale, and elliptic-shaped (Figure 2). While similar scars can arise from other sources, only those fitting this description were confidently identified as CCS, with ambiguous cases excluded (Figure 3).

2.3 | Individual Classification and Aerial-Identification Image Processing

Aerial top-down imagery of HBWs was processed using VideoLAN software version 3.0.16 (www.videolan.org). Individuals in still images were extracted and classified into two groups: 'lactating females' and 'others'. Lactating females were classified by the presence of a dependent calf in close proximity, with dependent calves defined as individuals measuring up to 50% of their mother's length (van Aswegen et al. 2025a). Calves were excluded from analyses, as their presence was captured through the identification of lactating females. Additionally, variation in scar healing and changes in tubercle visibility with growth may limit the consistency of calf identification. To ensure the method was tested under optimal conditions in this first application, we focused exclusively on adults with more stable and reliable identification features. Lactating females were analyzed separately due to their disproportionately low fluking rates and high energetic demands, making them the demographic most likely to benefit from improved identification rates. The 'others' category encompassed all age and sex classes except lactating females and their calves. These whales were pooled into a single group due to limited information on sex and sexual maturity.

We extracted two top-down images for each individual per sighting when possible: one optimizing TB visibility and the

other CCS visibility (if scars were present). During image selection, effort was made to minimize the effects of several factors that could obscure key identification features, including camera focus, whale orientation (i.e., head, pitch, and roll), and environmental conditions (i.e., surface glare, foam, and water distortion). In addition, images were selected where the animal was postured flat and near the water surface to minimize refraction effects. Although we did not apply a formal grading criteria, clear internal protocols were discussed and followed to extract the best image. In addition, screenshots were carried out by two trained analysts to minimize inconsistency.

2.4 | Developing an Aerial-Identification Catalog for Humpback Whales

We used I^{3}S, a freely available, partially automated recognition software (https://reijns.com/i3s/), to create an aerial-ID catalog of HBWs sampled via UAS. For aerial-ID, we selected a single top-down image per individual that clearly showed the dorsal surface and allowed placement of three consistent reference points. Among the four available I^{3}S packages, we selected I^{3}S Classic for its ability to annotate small features with easily distinguished spot centers (Van Tienhoven et al. 2007). This package requires three reference points that are consistently available and stable across images for effective comparison. For TB images, we used the medial-anterior point of the rostrum and both the left and right eyes as reference points (Figure 4). For CCS images, the medial-anterior point of the rostrum and the anterior insertion points of both the left and right pectoral fins served as reference points (Figure 4). As TBs are primarily located on the head anterior to the blowhole, and CCS are more widely distributed across the head and posterior to the blowhole, the triangular arrangement of reference points encompassed the majority of the annotation area for each feature (Van Tienhoven et al. 2007). While HBWs are known for their high maneuverability (Edel and Winn 1978; Nemeth et al. 2025), their cephalic region primarily consists of stiff skeletal bone, thereby limiting the effect of animal posture (e.g., body arching, flexing) on the distance between features, reducing error in match accuracy (Rosa et al. 2020).

Two trained analysts manually annotated images for both TB and CCS. Each analyst was assigned a separate, non-overlapping subset of images to maximize efficiency and avoid duplication of effort. Prior to full annotation, both analysts annotated a shared set of six images and compared results to standardize feature interpretation and reference point placement. In addition, both analysts independently documented their definitions of each annotation category and compared these to ensure a consistent understanding of feature classification. Any individual feature that did not meet our definition was not annotated, as were images with less than three annotation points (the minimum software requirement). Between 3 and 40 points were annotated for each image, creating a two-dimensional 'fingerprint file.' The software then compared these fingerprint files against others in the database (Figure 5). The database was organized into unique folders, each representing an individual whale and containing associated TB and/or CCS screenshots and fingerprint files.

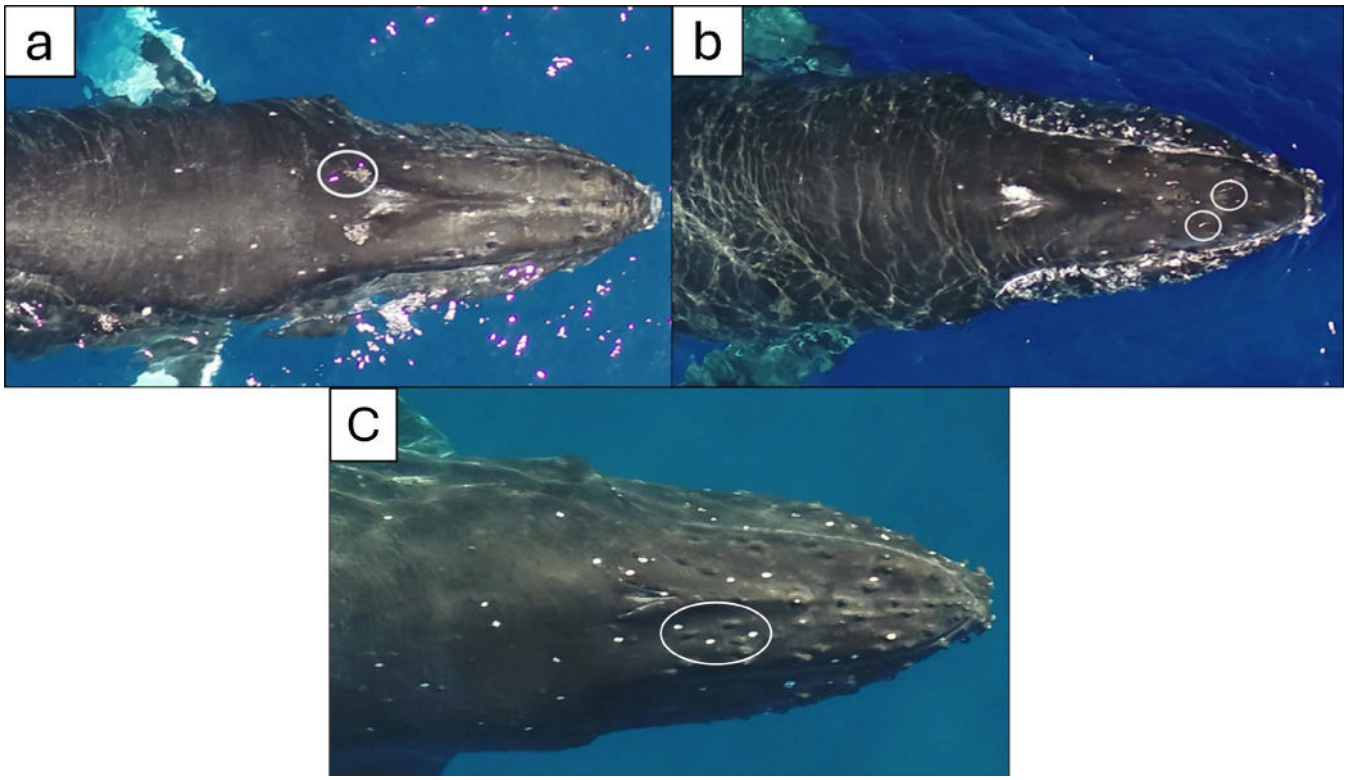

FIGURE 3 | Depictions of scars evaluated for cookiecutter shark scar (CCS) annotation. (a) The white circle highlights glare spots, which are distinguishable by their coloration but similar in size and shape to CCS; these were excluded from annotation. (b) The white circle shows scars that do not meet our criteria, lacking defined centers and thus also excluded from annotation. (c) The white circle shows a clear example of scars that did meet our criteria.

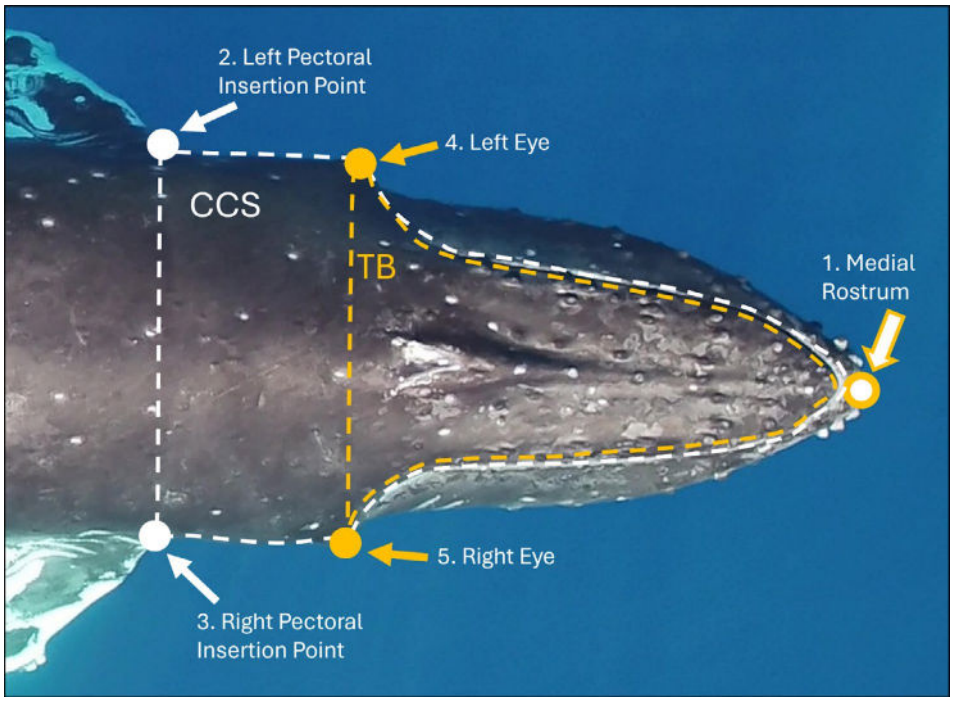

FIGURE 4 | A top-down drone screenshot of a humpback whale for aerial-identification annotation. The reference points for tubercle (TB) annotation are in orange and cookiecutter shark scar (CCS) are white: (1) medial rostrum, (2) left pectoral insertion point, (3) right pectoral insertion point, (4) right eye, (5) left eye. The dashed lines indicate the annotation regions for TB (orange) and CCS (white).

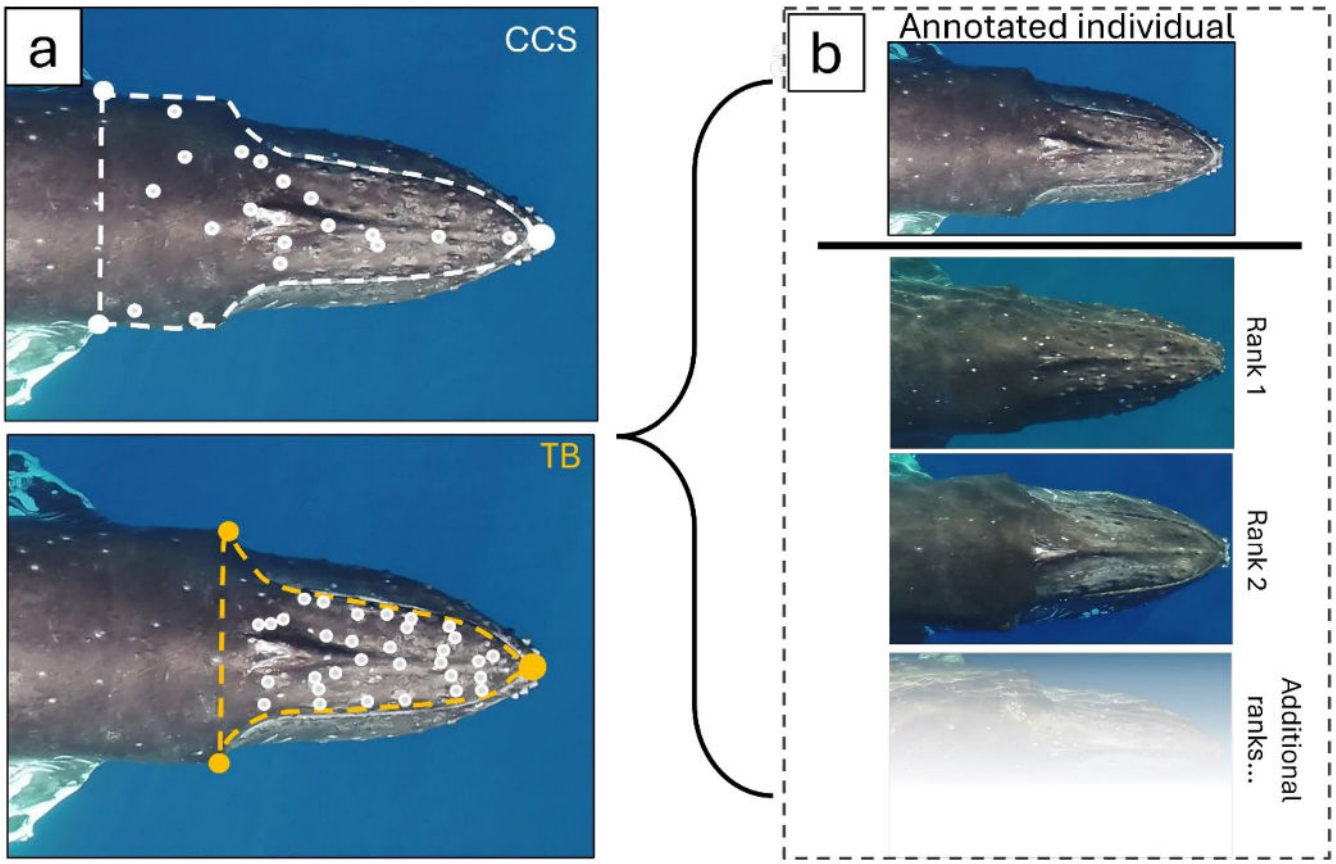

FIGURE 5 | Overview of our annotation and search methods in I^{3}S. (a) two annotated aerial-ID images of cookiecutter shark scars (CCS; white dashed line) and tubercles (TB; orange dashed line) where the large circles on the dashed line represent reference points and the white circles within the dashed lines represent annotated features. (b) shows the annotated image (above the black line) being searched against the database and I^{3}S-suggested matches (below the black line) ordered by recognition score.

Metadata were embedded in each annotated image to improve database searches and match accuracy. For example, each image was classified as TB or CCS, along with the individual's category (i.e., lactating female or other), thereby streamlining the search process and reducing the number of images searched against. TB and CCS images were processed separately in I^{3}S, with comparisons restricted to the same feature type to maintain consistency and optimize match quality. The annotated images were compared against the database using applied metadata. I^{3}S presented the top 50 candidate images for each query based on a recognition score, a ranking metric that orders potential matches from 1 (most likely match) to 50 (least likely among the returned set). The recognition score is calculated by aligning fingerprint files from two images using the three reference points and then comparing the relative distances between all annotated spot pairs in each image (Van Tienhoven et al. 2007). The score reflects the total distance between paired annotation points; lower scores indicate closer alignment of features and thus a higher likelihood of a match. The two analysts visually assessed the top-ranked suggested images to confirm matches. While I^{3}S returned up to 50 candidate images per query, a minimum of the top five suggestions was reviewed for each match attempt, with additional images assessed as needed based on match clarity and recognition scores. Matched images and their corresponding fingerprint files were added to the matched individual's folder, while unmatched images were placed into a new individual folder. If a fluke-ID image was linked to a specific aerial-ID image, all images within that individual's folder were subsequently associated with the same fluke-ID.

2.5 | Re-Sightings Using Traditional Fluke-ID

To establish a baseline for individual identification, we generated a fluke-ID catalog from tail fluke images collected during the study period. For each whale with a suitable fluke-ID photograph, we used the Happywhale platform (https://www.happywhale.com) to check for prior documentation of the individual. This involved uploading the fluke image and reviewing the top-ranked match suggestions returned by Happywhale's automated photo-identification algorithm, followed by visual confirmation to verify any potential matches. Happywhale assigns unique identification codes based on distinctive pigmentation and scarring patterns on the ventral fluke. We recorded the Happywhale code for each individual and cross-referenced these with other whales in our dataset. Individuals sharing the same code were classified as within-season re-sightings. We then compared the number of re-sightings identified using fluke-ID with those identified via aerial-ID.

2.6 | Multi-Year and Cross-Regional Matching of Tubercle Patterns

The aerial-ID workflow described for within-season analyses (Sections 2.2–2.4) was applied to test TB-based matching across years and regions. Individuals from Hawai‘i and Southeast Alaska (2018–2025) with ≥ 2 verified fluke-ID sightings in different seasons or years, from which a TB image could be extracted using the criteria described in Section 2.2, were included. As reproductive class can vary between years, metadata were omitted from annotated images and from subsequent catalog searches. A TB image from the first sighting was annotated and added to the within-season I^{3}S catalog, and the remaining verified images were annotated and searched against the same catalog. All matches were manually reviewed by one analyst to confirm matches, and any false positives were documented. Recognition scores and I^{3}S match ranks were recorded to compare multi-year and within-season performance.

2.7 | Statistical Analyses

To assess differences in re-sight rates between aerial-ID and fluke-ID, we used chi-squared tests for each demographic group. *Z*-tests were applied to compare both the total number of re-sights and the number of individuals re-sighted within each group. We also used *Z*-tests to evaluate differences in the number of assigned ID images captured by each method. Before conducting these tests, we confirmed that the sampling distributions approximated normality based on sample size and distribution characteristics. To compare recognition scores and mean suggested ranks between within-season and multi-year tubercle matches, we applied Mann–Whitney *U* tests and calculated the effect size.

3 | Results

3.1 | Within-Season Re-Sight Summary

From January 5 to March 30, 2022, we sampled 1498 HBWs (607 lactating females and 891 others) across 950 UAS flights, including repeated sightings of some individuals. Fluke-ID images were captured for 772 whales, while aerial-ID images with visible TB and/or CCS were extracted for 1437 whales. Aerial-ID resulted in more than 650 additional identifications compared to fluke-ID and improved both the number and proportion of whales re-sighted within the season. The longest re-sight interval also increased using aerial-ID (55 days vs. 49 days with fluke-ID; Table 1).

3.2 | Assessing Tubercles and Cookiecutter Scars for Within-Season Identification

Tubercle nodule patterns were more consistently visible for aerial-ID image annotations than CCS markings (TB, $n = 1334$; CCS, $n = 1191$). Tubercle nodule pattern images resulted in 52 more within–catalog matches than CCS images (Table 2). However, CCS images contributed 54 unique matches for individuals without a suitable TB image, highlighting their complementary role in aerial-ID. On average, matched CCS images appeared in the 1st or 2nd position of I^{3}S suggested results (mean rank = 1.11 ± 0.78), while TB images were typically ranked slightly lower (mean rank = 1.29 ± 1.65) (Table 2), indicating high match confidence for both features. Overall, 97.8% of the matched images were presented in the top three suggestions generated by I^{3}S (Table 2). TB markings were identifiable in re-sights up to 55 days apart, and CCS up to 52 days, representing the longest confirmed intervals for which these features remained distinguishable in matched individuals.

3.3 | Improved Within-Season Assignment of Identification Images Using Aerial-ID

By applying our aerial-ID method, we significantly improved the assignment of ID images compared to fluke-ID, particularly for lactating females (Figure 6). Using fluke-ID, we assigned ID images to 772 sampled individuals (237 lactating females and 535 others). In contrast, using aerial-ID, we assigned an ID image to 1437 sampled individuals, including 596 lactating females and 839 others. The proportion of individuals with an assigned ID increased from 39% to 98% among lactating females ($z = 28.81$, $p < 0.001$) and from 60% to 94% among others ($z = 21.64$, $p < 0.001$). Building on this improvement, we compared within-season re-sighting rates between methods.

3.4 | Improved Within-Season Re-Sighting of Individuals Using Aerial-ID

Using aerial-ID, we significantly increased the number of individuals re-sighted at least once within a season compared to fluke-ID. Using aerial-ID, we re-sighted 136 lactating females and 90 other individuals, compared to 45 and 46 using fluke-ID. These increases were significant for both lactating females ($z = -7.33$, $p < 0.001$) and others ($z = -3.93$, $p < 0.001$; $\chi^2(1) = 69.12$, $p < 0.001$; Figure 7a). We next examined whether aerial-ID also increased the total number of re-sights recorded across individuals.

Using aerial-ID, we significantly increased the total number of re-sight events compared to fluke-ID. We documented 164 total re-sights (76 lactating females and 88 others) using fluke-ID. In contrast, we yielded 372 re-sights, 227% more for lactating females ($n = 249$) and 40% more for others ($n = 123$) (Figure 7b) using aerial-ID. These increases were statistically significant for both groups (lactating females: $z = -13.57$, $p < 0.001$; others: $z = -3.35$, $p < 0.001$), and overall ($\chi^2(1) = 97.36$, $p < 0.001$).

TABLE 1 | Summary of identification metrics for humpback whales using fluke-ID and aerial-ID (tubercle and cookiecutter scar images), including the number of individuals sampled (including repeat sampling), identified, re-sighted, and the maximum time span between re-sightings during the 2022 study period.

	Fluke-ID	Aerial-ID
Number whales sampled including repeats	1498	1498
Number whales identified	772	1437
Individuals with ≥1 re-sighting	91	226
Total number of re-sights	162	372
Max time span between a re-sighted individual (days)	49	55

3.5 | Tubercles Remain Stable for Identification Across Multiple Years

Using fluke-ID, we identified 54 HBWs in the 2018–2025 catalog that were re-sighted in subsequent years, including 28 individuals matched between Southeast Alaska and Hawai'i. Using aerial-ID, we matched all 54 individuals, with 53 ranked in the top three suggestions and one ranked fourth (Table 3). Across all matches, the mean suggested rank was 1.13 ± 0.49, the mean recognition score was 5.30 ± 2.4, and re-sight intervals ranged from 210 days (~7 months) to 2373 days (~6 years, 6 months) (Table 4). Multi-year recognition scores were significantly higher than within-season scores (Mann–Whitney $U = 11{,}867$, $p = 0.0003$, $r = 0.18$), although the effect size was small. The mean suggested rank for multi-year matches (1.13) did not differ significantly from within-season matches (1.29) (Mann–Whitney $U = 1375$, $p = 0.478$, $r = 0.02$), indicating comparable ranking performance across timescales.

TABLE 2 | Matching performance for tubercles (TB) and cookiecutter shark scar (CCS) aerial-ID images, including the number of images annotated, the number of images matched, the mean rank position for matched images, the mean recognition score for matched images, and the percentage of matched images ranked within the top three suggestions.

	Number of images	Number of images matched within catalog	Mean rank	Mean recognition score	% of matched images in top three suggestions
TB: Lactating females	556	232	1.37	4.47	95.90
TB: Others	778	125	1.14	4.12	99.11
TB: Total	1334	357	1.29	4.35	96.99
CCS: Lactating females	567	233	1.09	15.09	98.71
CCS: Others	624	72	1.04	30.89	98.61
CCS: Total	1191	305	1.12	19.65	98.68
Total	2526	638	1.21	11.78	97.80

Note: Data are presented separately for lactating females, others, and combined totals.

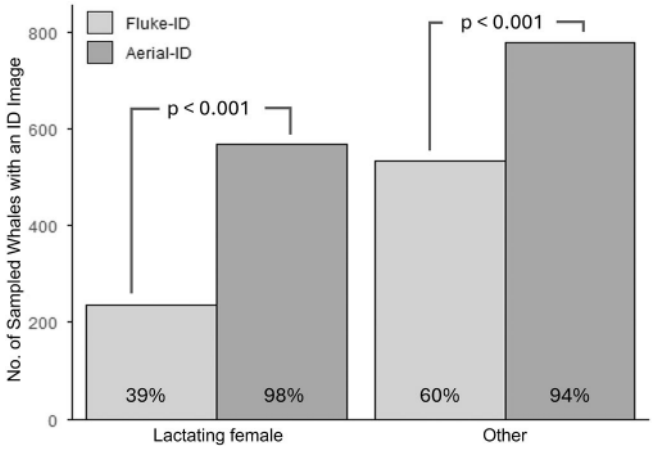

FIGURE 6 | Number of sampled individuals with an ID image using fluke-ID and aerial-ID methods for lactating females and others. Bars represent the total number of assigned IDs per demographic group (fluke-ID: $n = 237$ lactating females, 535 others; aerial-ID: $n = 596$ lactating females, 839 others), with percentages indicating the proportion of sampled individuals assigned an ID image by each method. *p*-values represent the significance between the methods for each demographic group performed by *z*-tests.

4 | Discussion

4.1 | Summary of Key Findings

This study tested the hypothesis that humpback whales can be individually identified using aerial imagery and found that aerial-ID outperforms traditional fluke-ID in image assignment and within-season re-sights, while also providing reliable matches across multiple years. Using fluke-ID, we recorded 76 total re-sightings for lactating females and 88 for others, compared to 249 and 123 using aerial-ID, representing increases of 227% and 40%, respectively. Similarly, the number of individuals sighted more than once increased substantially when using aerial-ID compared to fluke-ID: from 45 to 136 for lactating females (a 202% increase) and from 46 to 90 for other individuals (a 96% increase). These increases highlight the utility of aerial-ID as a complementary tool to fluke-ID, improving our ability to track individuals within seasons. Both TB and CCS contributed unique matches, each identifying over 50 individuals missed by the other. In confirmed within-season matches, TBs and CCS remained visible for up to 55 and 52 days, respectively, indicating that both features are reliable for short-term identification. While we did not

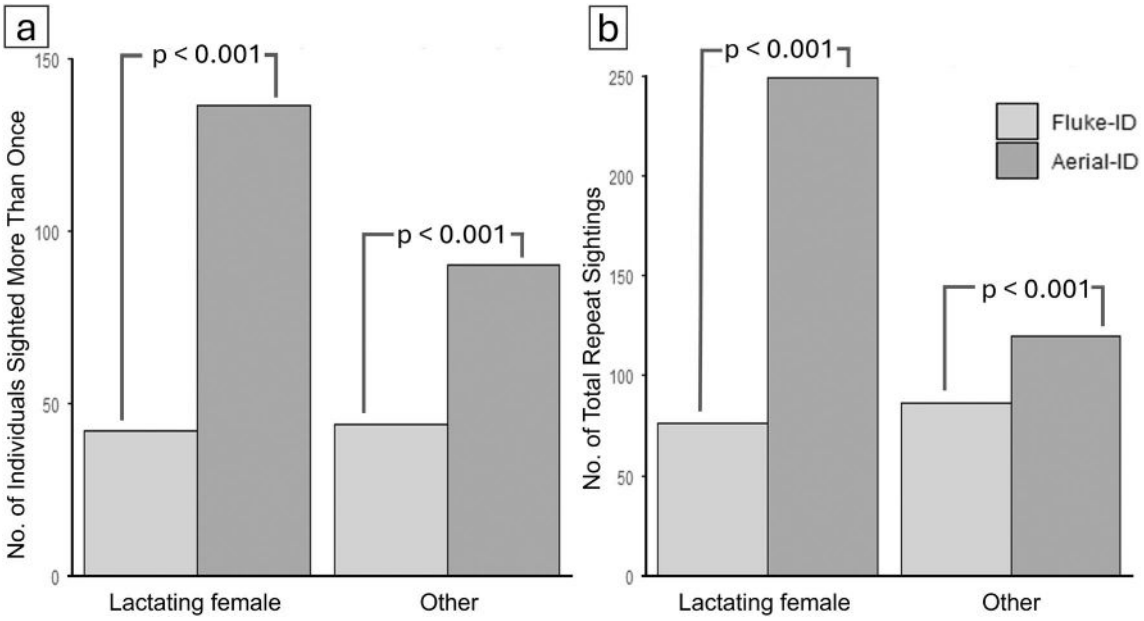

FIGURE 7 | (a) The number of individual whales sighted more than once using fluke-ID and aerial-ID for lactating females and others. Bars represent the total number of individuals with more than one sighting for each category using each method. *p*-values represent the significance between the methods for each category performed by *z*-tests. (b) The total number of repeat sightings documented for lactating females and others using fluke-ID and aerial-ID methods. Bars represent the total number of re-sights for each category using the two identification methods. *p*-values represent the significance between the methods for each category performed by *z*-tests.

TABLE 3 | Matching performance for tubercle aerial-ID images in multi-year analysis, including the number of images searched in the catalog, the number of matches, the mean rank position for matched images, the mean recognition score, and the percentage of matched images ranked within the top three suggestions.

	Number of images	Number of images matched within catalog	Mean rank	Mean recognition score	% of matched images in top three suggestions
TB	54	54	1.13 ± 0.49	5.30 ± 2.4	98.1

TABLE 4 | Summary of re-sight intervals for 54 humpback whales matched using tubercle (TB) aerial-ID between 2018 and 2025.

	Minimum re-sight interval	Maximum re-sight interval	Mean ± SD re-sight interval	Median re-sight interval
Number of days (years)	210 (0.6)	2737 (6.5)	1229 ± 584 (3.4 ± 1.6)	1112 (3.0)

Note: Values are presented in days, with equivalent years shown in parentheses.

assess feature degradation for individuals or validate matches using fluke-ID, these intervals suggest both features were sufficiently stable for short-term identification.

We extended this approach to a multi-year dataset to test if TB patterns remain stable over longer intervals. Using fluke-ID, we identified 54 individuals photographed between 2018 and 2025, including 28 matched between Southeast Alaska and Hawai'i. Using our aerial-ID method, all 54 individuals were successfully matched, with the longest re-sight spanning 2737 days (6.5 years) and over 98% ranked within the top three algorithm suggestions. Recognition scores were statistically higher for multi-year matches than within-season matches (Mann–Whitney U test, $p = 0.0003$), but the small effect size ($r = 0.18$) indicates that the magnitude of this difference was minimal. Consistent with this, mean rank position did not differ significantly between timescales (1.07 vs. 1.29; $p = 0.478$), suggesting that the matching algorithm performed similarly whether images were taken weeks or years apart. These findings indicate that TB patterns remain stable over a 6-year interval. This supports their use for both short- and long-term individual identification and indicates strong potential for reliable application over longer timescales.

Capturing fluke images was likely limited by the behavior of different demographic groups on the breeding grounds. Lactating females fluked infrequently, likely to conserve energy while resting and due to their use of shallow waters, which may reduce male harassment and limit deep diving (Cartwright et al. 2012; Craig et al. 2014; Currie et al. 2018; Bejder et al. 2019; Pack et al. 2022). Most individuals in the 'other' category are likely males, given the male-biased sex ratio on the Hawaiian breeding grounds (Clapham 1996). Their frequent engagement in energetically costly, competitive surface behaviors while fasting may both reduce fluking rates and make available flukes more difficult to photograph (Christiansen, Dujon, et al. 2016; Christiansen, Rojano-Doñate, et al. 2016; Tyack and Whitehead 1983). In contrast, aerial-ID was less constrained by behavioral variability among demographic groups and supported higher rates of individual identification.

While TBs demonstrated high stability across years, CCS may be less reliable over similar intervals. In killer whales, CCS typically heals within approximately 150 days (Dwyer 2011), and similar healing is likely in HBWs, reducing the duration over which scars remain distinctive. However, scars have persisted for many months in short-finned pilot whales (*Globicephala macrorhynchus*), with some individuals carrying over 30 distinct marks and scarring evident year-round, suggesting that healed wounds may remain visible for extended periods (Walker-Milne et al. 2025). Nevertheless, cookiecutter shark prevalence varies across populations, common in regions such as Hawai'i and the South Pacific but notably scarce in higher-latitude areas and shallow coastal zones, limiting their utility for broader application (Best and Photopoulou 2016).

4.2 | Implications for Humpback Whale Research

Aerial-ID complements traditional photo-ID techniques by addressing limitations of both fluke-ID and dorsal fin ID, particularly for demographic groups such as lactating females. Dorsal fin ID, while extremely useful, is limited by variable distinctiveness and the need for high-quality lateral images. In cases where visual ID is unsuccessful, genetic matching can provide accurate identifications but is costly, invasive, and less accessible. By leveraging UAS imagery collected for body condition assessments, aerial-ID maximizes data yield while occupying a unique position on the accessibility–reliability spectrum, filling critical gaps left by conventional approaches.

The application of aerial-ID, both to existing archives and future datasets, opens opportunities to shift from cross-sectional snapshots toward longitudinal records that track individuals over time. While cross-sectional datasets provide useful population-level overviews, they are limited in their ability to track individual variability or responses to ecological and anthropogenic disturbances. In contrast, longitudinal data based on re-sightings allow researchers to detect changes in body condition or injury status, uncover causal ecological relationships, and track demographic and behavioral dynamics over time. These data offer insight into individual variation and temporal dynamics, essential for understanding physiological responses, resilience to disturbance, and demographic patterns. Aerial-ID supports these assessments by increasing the number and frequency of individual re-sightings, particularly for lactating females.

One application of longitudinal data is monitoring body condition, a key physiological determinant of reproductive success and resilience to disturbance, yet detecting changes requires repeated observations of known individuals across time (Christiansen, Dujon, et al. 2016; Christiansen, Rojano-Doñate, et al. 2016; Christiansen, Nielsen, et al. 2020; Christiansen, Dawson, et al. 2020, Christiansen et al. 2023; Pirotta et al. 2018). However, such longitudinal assessments have traditionally been limited by infrequent re-sightings, particularly for lactating females (Bierlich et al. 2022; Christiansen, Dujon, et al. 2016; Christiansen, Rojano-Doñate, et al. 2016). Aerial-ID in conjunction with fluke-ID improves this by increasing both the number of individuals re-sighted and the number of times each is observed. For instance, van Aswegen et al. (2025a) demonstrated that repeat aerial and fluke-ID sightings enabled fine-scale estimates of maternal energy expenditure and calf growth, linking maternal size and condition to offspring fitness. This resolution

moves beyond population-level averages, supporting more precise individual-level bioenergetic estimates and enhancing our ability to detect physiological responses to disturbance. When applied across multiple years and across both breeding and feeding grounds, aerial-ID in combination with fluke-ID allows repeated measurements of the same individuals between seasons and across years. These repeated measures can reveal long-term body condition trends tied to climate, prey availability, and other environmental drivers, linking individual health to large-scale ecosystem change across the migratory cycle.

Beyond health, improvements in detection and re-sighting frequency also have important implications for population-level modeling. Mark-recapture models are among the most widely used tools for estimating cetacean population parameters such as abundance, survival, and movement rates (Hammond et al. 2021). These metrics are foundational for assessing population health and forecasting trajectories. More advanced frameworks, such as multistate, spatially explicit, or robust design models, can yield rich insights into demographic and temporal variation in population parameters, but they are inherently data-hungry and often limited by sparse and uneven re-sighting data. Aerial-ID helps address these challenges by improving coverage and re-sighting rates, thereby reducing detection bias and strengthening the consistency of individual identifications. Comparable success has already been demonstrated in North Atlantic right whales, where aerial imagery of callosity patterns has enabled robust mark–recapture analyses (Crowe et al. 2021), highlighting the broader utility of aerial-based identification for both short-term and long-term monitoring in HBWs.

Enhanced individual recognition enables researchers to track behavioral and spatial patterns across the breeding season and, when extended over multiple years, to detect shifts in habitat use and evaluate site fidelity at the individual level. Previous studies have shown that mother–calf pairs in Hawai'i often avoid nearshore areas, likely balancing disturbance risk against male harassment (Cartwright et al. 2012; Craig et al. 2014; Pack et al. 2022). However, these studies relied on cross-sectional data, limiting their ability to assess if individuals consistently use or shift habitat over time. Aerial-ID addresses this gap by allowing repeated identification of individuals within and across years, including across the species' migratory range, which can span thousands of kilometers. This capability supports individual-level monitoring of habitat use, revealing demographic differences in site fidelity and behavioral plasticity. Such fine-scale, long-term tracking is particularly valuable for wide-ranging species like HBWs, whose movements cross multiple management jurisdictions and habitat types, making coordinated conservation challenging. By providing a finer-scale, long-term view of individual habitat use across regions, aerial-ID can help identify high-use areas and conflict zones with greater precision, strengthening the basis for spatial management and targeted conservation at both local and migratory scales.

4.3 | Future Directions

While fluke-ID contributes extensive life history data from historical databases, aerial-ID complements it by expanding coverage to individuals less likely to fluke out, together enabling more inclusive and comprehensive monitoring. Building on the findings of this study, future research should determine whether tubercle patterns remain stable beyond the timescales tested here and how their persistence compares with fluke-ID. If confirmed, this stability could enable decades-long individual tracking, revealing detailed calving histories, site fidelity, and body condition trends in response to environmental change. In addition, extending this method to include calves, particularly by testing the reliability of TBs across developmental stages, could fill critical gaps in our understanding of survival, recruitment, and population dynamics.

A primary limitation of partially automated systems like I^3S is their reliance on manual annotation and matching, which are inherently slower and more variable than fully automated approaches. While we applied consistent internal criteria, distinguishing between tubercles and cookiecutter scars can be subjective, particularly when features are faint, overlapping, or distorted by glare, an issue that may be amplified across analysts or research groups (Kniest et al. 2010). As UAS-derived imagery becomes increasingly common, integrating modern AI-based pattern recognition into aerial-ID workflows offers a path toward faster, more scalable, and less biased identification. Recent advances in AI-driven identification methods have already outperformed traditional approaches across diverse species and datasets (Cheeseman et al. 2022; Patton et al. 2023, 2025), signaling a rapid shift in the field. Continued development and refinement of these tools will be essential for unlocking the full potential of aerial-ID in long-term, individual-based monitoring.

5 | Conclusion

We demonstrate that our novel aerial-ID approach significantly increases the number of individuals identified and total resight rates of HBWs compared to fluke-ID. Both TB and CCS supported reliable within-season identification, while TBs also demonstrated stability and utility for matches spanning multiple years. By enabling higher-resolution individual-level tracking, aerial-ID has the potential to support a broad range of research, including studies on energetics, habitat use, and population monitoring. Importantly, aerial-ID complements fluke-ID by improving the identification of individuals that rarely fluke out, such as lactating females, thereby broadening demographic coverage and enhancing the effectiveness of individual-based monitoring. When applied over extended timeframes and across breeding and feeding grounds, aerial-ID facilitates long-term, cross-regional studies that can link calving histories, site fidelity, and body condition to environmental change. Given recent advances in machine learning, we recommend future integration of AI with aerial-ID methods to improve efficiency, scalability, and accuracy while reducing human error. Ultimately, aerial-ID represents a powerful addition to the toolkit for non-invasive population monitoring and informing conservation management.

Author Contributions

L.I.E., M.v.A., and S.F. conceived the study. L.B., M.v.A., J.J.C., S.H.S.. and A.S., secured funding for the fieldwork. M.v.A., L.I.E., J.J.C., L.B.,

S.F., and S.H.S. carried out fieldwork. Data processing was carried out by L.I.E. and S.F. Statistical analysis and interpretation were carried out by L.I.E. and S.F. L.I.E. wrote the manuscript with input from L.B. All authors reviewed and commented on the manuscript.

Acknowledgments

We thank the numerous research assistants who helped with fieldwork and data processing. We are grateful to Abigail Machernis, Grace Olson, Florence Sullivan, Elizabeth Beato, Jessie Hoffman, and Dana Bloch for their dedication and support toward this study's data collection. We thank Nicholas Nemeth for the initial translation of the English abstract to Hawaiian and Ekolu Kelley for verification and editing. We also thank PacWhale Eco-Adventures, Christina Lovitt, and Emma Nelson (Maui Ocean Adventures), Lee James (Ultimate Whale Watch), and the Guth family for their logistical support. Data were collected under National Marine Fisheries Service permits 21476 and 20311 and with approval from the University of Hawai'i Institutional Animal Care and Use Committee (18-2971). Qualified Federal Aviation Administration Part 107 drone pilots operated the UAS. This paper represents HIMB and SOEST contribution nos. 2006 and 11989, respectively.

Conflicts of Interest

The authors declare no conflicts of interest.

Data Availability Statement

The data that support the findings of this study are available from the corresponding author upon reasonable request.

References

Bejder, L., D. Fletcher, and S. Bräger. 1998. "A Method for Testing Association Patterns of Social Animals." *Animal Behaviour* 56, no. 3: 719–725. https://doi.org/10.1006/anbe.1998.0802.

Bejder, L., S. Videsen, L. Hermannsen, M. Simon, D. Hanf, and P. T. Madsen. 2019. "Low Energy Expenditure and Resting Behaviour of Humpback Whale Mother-Calf Pairs Highlights Conservation Importance of Sheltered Breeding Areas." *Scientific Reports* 9, no. 1: 771. https://doi.org/10.1038/s41598-018-36870-7.

Best, P. B., and T. Photopoulou. 2016. "Identifying the 'Demon Whale-Biter': Patterns of Scarring on Large Whales Attributed to a Cookie-Cutter Shark *Isistius* sp." *PLoS One* 11, no. 4: e0152643. https://doi.org/10.1371/journal.pone.0152643.

Bichell, L. M. V., E. Krzyszczyk, E. M. Patterson, and J. Mann. 2018. "The Reliability of Pigment Pattern-Based Identification of Wild Bottlenose Dolphins." *Marine Mammal Science* 34, no. 1: 113–124. https://doi.org/10.1111/mms.12440.

Bierlich, K. C., J. Hewitt, R. S. Schick, et al. 2022. "Seasonal Gain in Body Condition of Foraging Humpback Whales Along the Western Antarctic Peninsula." *Frontiers in Marine Science* 9: 1036860. https://doi.org/10.3389/fmars.2022.1036860.

Blount, D., S. Gero, J. Van Oast, et al. 2022. "Flukebook: An Open-Source AI Platform for Cetacean Photo Identification." *Mammalian Biology* 102, no. 3: 1005–1023. https://doi.org/10.1007/s42991-021-00221-3.

Bogucki, R., M. Cygan, C. B. Khan, M. Klimek, J. K. Milczek, and M. Mucha. 2019. "Applying Deep Learning to Right Whale Photo Identification." *Conservation Biology* 33, no. 3: 676–684. https://doi.org/10.1111/cobi.13226.

Borchers, D., G. Distiller, R. Foster, B. Harmsen, and L. Milazzo. 2014. "Continuous-Time Spatially Explicit Capture–Recapture Models, With an Application to a Jaguar Camera-Trap Survey." *Methods in Ecology and Evolution* 5, no. 7: 656–665. https://doi.org/10.1111/2041-210X.12196.

Brooks, K., D. Rowat, S. J. Pierce, D. Jouannet, and M. Vely. 2010. "Seeing Spots: Photo-Identification as a Regional Tool for Whale Shark Identification." *Western Indian Ocean Journal of Marine Science* 9, no. 2: 185–194.

Calambokidis, J., E. A. Falcone, T. J. Quinn, et al. 2008. "SPLASH: Structure of Populations, Levels of Abundance and Status of Humpback Whales in the North Pacific." Final Report for Contract AB133F-03-RP-00078. Cascadia Research Collective.

Cartwright, R., B. Gillespie, K. LaBonte, et al. 2012. "Between a Rock and a Hard Place: Habitat Selection in Female-Calf Humpback Whale (*Megaptera novaeangliae*) Pairs on the Hawaiian Breeding Grounds." *PLoS One* 7, no. 5: e38004. https://doi.org/10.1371/journal.pone.0038004.

Cheeseman, T., J. Barlow, J. M. Acebes, et al. 2024. "Bellwethers of Change: Population Modelling of North Pacific Humpback Whales From 2002 Through 2021 Reveals Shift From Recovery to Climate Response." *Royal Society Open Science* 11, no. 2: 231462. https://doi.org/10.1098/rsos.231462.

Cheeseman, T., K. Southerland, J. Park, et al. 2022. "Advanced Image Recognition: A Fully Automated, High-Accuracy Photo-Identification Matching System for Humpback Whales." *Mammalian Biology* 102, no. 3: 915–929. https://doi.org/10.1007/s42991-021-00180-9.

Cheney, B. J., J. Dale, P. M. Thompson, and N. J. Quick. 2022. "Spy in the Sky: A Method to Identify Pregnant Small Cetaceans." *Remote Sensing in Ecology and Conservation* 8, no. 4: 492–505. https://doi.org/10.1002/rse2.258.

Christiansen, F., S. M. Dawson, J. W. Durban, et al. 2020. "Population Comparison of Right Whale Body Condition Reveals Poor State of the North Atlantic Right Whale." *Marine Ecology Progress Series* 640: 1–16. https://doi.org/10.3354/meps13299.

Christiansen, F., A. M. Dujon, K. R. Sprogis, J. P. Y. Arnould, and L. Bejder. 2016. "Noninvasive Unmanned Aerial Vehicle Provides Estimates of the Energetic Cost of Reproduction in Humpback Whales." *Ecosphere* 7, no. 10: e01468. https://doi.org/10.1002/ecs2.1468.

Christiansen, F., M. L. K. Nielsen, C. Charlton, L. Bejder, and P. T. Madsen. 2020. "Southern Right Whales Show no Behavioral Response to Low Noise Levels From a Nearby Unmanned Aerial Vehicle." *Marine Mammal Science* 36, no. 3: 953–963. https://doi.org/10.1111/mms.12699.

Christiansen, F., L. Rojano-Doñate, P. T. Madsen, and L. Bejder. 2016. "Noise Levels of Multi-Rotor Unmanned Aerial Vehicles With Implications for Potential Underwater Impacts on Marine Mammals." *Frontiers in Marine Science* 3: 277. https://doi.org/10.3389/fmars.2016.00277.

Christiansen, F., K. R. Sprogis, M. L. K. Nielsen, M. Glarou, and L. Bejder. 2023. "Energy Expenditure of Southern Right Whales Varies With Body Size, Reproductive State and Activity Level." *Journal of Experimental Biology* 226, no. 13: jeb245137. https://doi.org/10.1242/jeb.245137.

Clapham, P. J. 1996. "The Social and Reproductive Biology of Humpback Whales: An Ecological Perspective." *Mammal Review* 26, no. 1: 27–49. https://doi.org/10.1111/j.1365-2907.1996.tb00145.x.

Clapham, P. J., L. S. Baraff, C. A. Carlson, et al. 1993. "Seasonal Occurrence and Annual Return of Humpback Whales, *Megaptera novaeangliae*, in the Southern Gulf of Maine." *Canadian Journal of Zoology* 71, no. 2: 440–443. https://doi.org/10.1139/z93-063.

Craig, A. S., and L. M. Herman. 1997. "Sex Differences in Site Fidelity and Migration of Humpback Whales (*Megaptera novaeangliae*) to the Hawaiian Islands." *Canadian Journal of Zoology* 75, no. 11: 1923–1933. https://doi.org/10.1139/z97-822.

Craig, A. S., L. M. Herman, A. A. Pack, and J. O. Waterman. 2014. "Habitat Segregation by Female Humpback Whales in Hawaiian Waters: Avoidance of Males?" *Behaviour* 151, no. 5: 613–631. https://doi.org/10.1163/1568539X-00003151.

Crowe, L. M., M. W. Brown, P. J. Corkeron, et al. 2021. "In Plane Sight: A Mark-Recapture Analysis of North Atlantic Right Whales in the Gulf of St. Lawrence." *Endangered Species Research* 46: 227–251. https://doi.org/10.3354/esr01156.

Currie, J. J., S. H. Stack, J. A. McCordic, and J. Roberts. 2018. "Utilizing Occupancy Models and Platforms-of-Opportunity to Assess Area Use of Mother-Calf Humpback Whales." *Open Journal of Marine Science* 8, no. 2: 276–292. https://doi.org/10.4236/ojms.2018.82014.

Durban, J. W., H. Fearnbach, L. G. Barrett-Lennard, W. L. Perryman, and D. J. Leroi. 2015. "Photogrammetry of Killer Whales Using a Small Hexacopter Launched at Sea." *Journal of Unmanned Vehicle Systems* 3, no. 3: 131–135. https://doi.org/10.1139/juvs-2015-0020.

Dwyer, S. 2011. "Cookie Cutter Shark (*Isistius sp.*) Bites on Cetaceans, With Particular Reference to Killer Whales (*Orcinus orca*)." *Aquatic Mammals* 37, no. 2: 111–138. https://doi.org/10.1578/AM.37.2.2011.111.

Edel, R. K., and H. E. Winn. 1978. "Observations on Underwater Locomotion and Flipper Movement of the Humpback Whale *Megaptera novaeangliae*." *Marine Biology* 48, no. 3: 279–287. https://doi.org/10.1007/BF00397155.

Fleming, A., and J. Jackson. 2011. *Global Review of Humpback Whales (Megaptera novaeangliae). NOAA Technical Memorandum NMFS*. US National Oceanic and Atmospheric Administration. https://doi.org/10.1007/978-1-4684-2985-5_2.

Frasier, T. R., P. K. Hamilton, M. W. Brown, S. D. Kraus, and B. N. White. 2009. "Sources and Rates of Errors in Methods of Individual Identification for North Atlantic Right Whales." *Journal of Mammalogy* 90, no. 5: 1246–1255. https://doi.org/10.1644/08-MAMM-A-328.1.

Gabriele, C. M., J. L. Neilson, J. M. Straley, C. S. Baker, J. A. Cedarleaf, and J. F. Saracco. 2017. "Natural History, Population Dynamics, and Habitat Use of Humpback Whales Over 30 Years on an Alaska Feeding Ground." *Ecosphere* 8, no. 1: e01641. https://doi.org/10.1002/ecs2.1641.

Hammond, P. S., T. B. Francis, D. Heinemann, et al. 2021. "Estimating the Abundance of Marine Mammal Populations." *Frontiers in Marine Science* 8: 735770. https://doi.org/10.3389/fmars.2021.735770.

Hartman, K., P. van der Harst, and R. Vilela. 2020. "Continuous Focal Group Follows Operated by a Drone Enable Analysis of the Relation Between Sociality and Position in a Group of Male Risso's Dolphins (*Grampus griseus*)." *Frontiers in Marine Science* 7: 283. https://doi.org/10.3389/fmars.2020.00283.

Hook, S. A., C. McMurray, D. M. Ripley, et al. 2019. "Recognition Software Successfully Aids the Identification of Individual Small-Spotted Catsharks (*Scyliorhinus canicula*) During Their First Year of Life." *Journal of Fish Biology* 95, no. 6: 1465–1470. https://doi.org/10.1111/jfb.14166.

Hoyos-Padilla, M., Y. P. Papastamatiou, J. O'Sullivan, and C. G. Lowe. 2013. "Observation of an Attack by a Cookiecutter Shark (*Isistius brasiliensis*) on a White Shark (*Carcharodon carcharias*)." *Pacific Science* 67, no. 1: 129–134. https://doi.org/10.2984/67.1.10.

Jahn, A. E., and R. L. Haedrich. 1988. "Notes on the Pelagic Squaloid Shark *Isistius brasiliensis*." *Biological Oceanography* 5, no. 4: 297–309.

Katona, S., B. Baxter, O. Brazier, S. Kraus, J. Perkins, and H. Whitehead. 1979. "Identification of Humpback Whales by Fluke Photographs." In *Behavior of Marine Animals*, edited by H. E. Winn and B. L. Olla, 33–44. Plenum Press. https://doi.org/10.1007/978-1-4684-2985-5_2.

Katona, S. K., and H. P. Whitehead. 1981. "Identifying Humpback Whales Using Their Natural Markings." *Polar Record* 20, no. 128: 439–444. https://doi.org/10.1017/S003224740000365X.

Kaufman, G., M. Smultea, and P. Forestell. 1987. "Use of Lateral Body Pigmentation Patterns for Photographic Identification of East Australian (Area V) Humpback Whales." *Cetus* 7: 5–13.

Kniest, E., D. Burns, and P. Harrison. 2010. "Fluke Matcher: A Computer-Aided Matching System for Humpback Whale (*Megaptera novaeangliae*) Flukes." *Marine Mammal Science* 26: 744–756. https://doi.org/10.1111/j.1748-7692.2009.00368.x.

Koski, W. R., G. Gamage, A. R. Davis, T. Mathews, B. LeBlanc, and S. H. Ferguson. 2015. "Evaluation of UAS for Photographic Re-Identification of Bowhead Whales, *Balaena mysticetus*." *Journal of Unmanned Vehicle Systems* 3, no. 1: 22–29. https://doi.org/10.1139/juvs-2014-0014.

Ling, J. K. 1977. "Vibrissae of Marine Mammals." In *Functional Anatomy of Marine Animals*, edited by R. J. Harrison, 387–415. Academic Press.

Martins, M. C. I., C. Miller, P. Hamilton, J. Robbins, D. P. Zitterbart, and M. Moore. 2020. "Respiration Cycle Duration and Seawater Flux Through Open Blowholes of Humpback and North Atlantic Right Whales." *Marine Mammal Science* 36, no. 4: 1160–1179. https://doi.org/10.1111/mms.12703.

McPherson, L., J. Badger, K. Fertitta, M. Gordanier, C. Nemeth, and L. Bejder. 2024. "Quantifying the Abundance and Survival Rates of Island-Associated Spinner Dolphins Using a Multi-State Open Robust Design Model." *Scientific Reports* 14, no. 1: 14764. https://doi.org/10.1038/s41598-024-64220-3.

Mercado, E. 2014. "Short Note Tubercles: What Sense Is There?" *Aquatic Mammals* 40, no. 1: 95–103. https://doi.org/10.1578/AM.40.1.2014.95.

Moreira-Mendieta, A., D. O. Urquía, P. Asadobay, and D. Páez-Rosas. 2024. "Evidence of a Predatory Interaction of a Cookiecutter Shark (*Isistius brasiliensis*) on Galapagos Fur Seals (*Arctocephalus galapagoensis*)." *Aquatic Mammals* 50, no. 2: 127–133. https://doi.org/10.1578/AM.50.2.2024.127.

Nakano, H., and K. Nagasawa. 1996. "Distribution of Pelagic Elasmobranchs Caught by Salmon Research Gillnets in the North Pacific." *Fisheries Science* 62, no. 6: 860–865. https://doi.org/10.2331/fishsci.62.860.

Napoli, C., N. Hirtle, J. Stepanuk, et al. 2024. "Drone-Based Photogrammetry Reveals Differences in Humpback Whale Body Condition and Mass Across North Atlantic Foraging Grounds." *Frontiers in Marine Science* 11: 1336455. https://doi.org/10.3389/fmars.2024.1336455.

Nemeth, C., W. T. Gough, P. S. Segre, et al. 2025. "The Key to Bubble-Net Feeding: How Humpback Whale Morphology Functionally Differs From Other Baleen Whales." *Journal of Experimental Biology* 228, no. 16: jeb249607. https://doi.org/10.1242/jeb.249607.

Niella, Y. V., L. A. G. Duarte, V. R. Bandeira, O. Crespo, D. Beare, and F. H. V. Hazin. 2018. "Cookie-Cutter Shark *Isistius spp*. Predation Upon Different Tuna Species From the South-Western Atlantic Ocean." *Journal of Fish Biology* 92, no. 4: 1082–1089. https://doi.org/10.1111/jfb.13569.

O'Callaghan, S. A., F. Al Abbar, H. Costa, R. Prieto, M. Gammell, and J. O'Brien. 2024. "Aerial Photo-Identification of Sperm Whales (*Physeter macrocephalus*)." *Aquatic Mammals* 50, no. 6: 479–494. https://doi.org/10.1578/AM.50.6.2024.479.

Pack, A. A., J. O. Waterman, and A. S. Craig. 2022. "Diurnal Increases in Depths of Humpback Whale (*Megaptera novaeangliae*) Mother-Calf Pods Off West Maui, Hawai'i: A Response to Vessels?" *Marine Mammal Science* 38, no. 4: 1340–1356. https://doi.org/10.1111/mms.12926.

Patton, P. T., T. Cheeseman, K. Abe, et al. 2023. "A Deep Learning Approach to Photo–Identification Demonstrates High Performance on Two Dozen Cetacean Species." *Methods in Ecology and Evolution* 14, no. 10: 2611–2625. https://doi.org/10.1111/2041-210X.14167.

Patton, P. T., K. Pacifici, R. W. Baird, et al. 2025. "Optimizing Automated Photo Identification for Population Assessments." *Conservation Biology* 39: e14436. https://doi.org/10.1111/cobi.14436.

Pirotta, E., C. G. Booth, D. P. Costa, et al. 2018. "Understanding the Population Consequences of Disturbance." *Ecology and Evolution* 8, no. 19: 9934–9946. https://doi.org/10.1002/ece3.4458.

Reeb, D., P. B. Best, and S. H. Kidson. 2007. "Structure of the Integument of Southern Right Whales, *Eubalaena australis*." *Anatomical Record* 290: 596–613. https://doi.org/10.1002/ar.20535.

Rice, M., C. Carlson, K. Chu, W. Dolphin, and H. Whitehead. 1987. "Are Humpback Whale Population Estimates Being Biased by Sexual Differences in Fluking Behavior?" *Report of the International Whaling Commission* 37: 333–335.

Rosa, G., F. Guillaud, P. Priol, and J. Renet. 2020. "Parameter Affecting the I3S Algorithm Reliability: How Does Correcting for Body Curvature Affect Individual Recognition?" *Wildlife Research* 48, no. 1: 38–43. https://doi.org/10.1071/WR19238.

Ryan, K. P., S. H. Ferguson, W. R. Koski, B. G. Young, J. D. Roth, and C. A. Watt. 2022. "Use of Drones for the Creation and Development of a Photographic Identification Catalogue for an Endangered Whale Population." *Arctic Science* 8, no. 4: 1191–1201. https://doi.org/10.1139/as-2021-0047.

Sacchi, R., S. Scali, D. Pellitteri-Rosa, et al. 2010. "Photographic Identification in Reptiles: A Matter of Scales." *Amphibia-Reptilia* 31, no. 4: 489–502. https://doi.org/10.1163/017353710X521546.

Schevill, W. E., and R. H. Backus. 1960. "Daily Patrol of a *Megaptera*." *Journal of Mammalogy* 41, no. 2: 279–281. https://doi.org/10.2307/1376380.

Stevick, P. T., J. Allen, P. J. Clapham, et al. 2003. "North Atlantic Humpback Whale Abundance and Rate of Increase Four Decades After Protection From Whaling." *Marine Ecology Progress Series* 258: 263–273. https://doi.org/10.3354/meps258263.

Stewart, J. D., J. W. Durban, A. R. Knowlton, et al. 2021. "Decreasing Body Lengths in North Atlantic Right Whales." *Current Biology* 31, no. 14: 3174–3179. https://doi.org/10.1016/j.cub.2021.04.067.

Taberlet, P., and G. Luikart. 1999. "Non-Invasive Genetic Sampling and Individual Identification." *Biological Journal of the Linnean Society* 68, no. 1–2: 41–55. https://doi.org/10.1111/j.1095-8312.1999.tb01157.x.

Taylor, B. L., and T. Gerrodette. 1993. "The Uses of Statistical Power in Conservation Biology: The Vaquita and Northern Spotted Owl." *Conservation Biology* 7, no. 3: 489–500. https://doi.org/10.1046/j.1523-1739.1993.07030489.x.

Tomilin, A. G. 1967. *Mammals of the U.S.S.R. and Adjacent Countries: Vol. IX. Cetacea*. Israel Program for Scientific Translations.

Tyack, P., and H. Whitehead. 1983. "Male Competition in Large Groups of Wintering Humpback Whales." *Behaviour* 83, no. 1–2: 132–154. https://doi.org/10.1163/156853982X00067.

van Aswegen, M., A. Szabo, J. J. Currie, et al. 2025a. "Maternal Investment, Body Condition and Calf Growth in Humpback Whales." *Journal of Physiology* 603, no. 2: 551–578. https://doi.org/10.1113/JP287379.

van Aswegen, M., A. Szabo, J. J. Currie, et al. 2025b. "Energetic Cost of Gestation and Prenatal Growth in Humpback Whales." *Journal of Physiology* 603, no. 2: 529–550. https://doi.org/10.1113/JP287304.

Van Tienhoven, A. M., J. E. Den Hartog, R. A. Reijns, and V. M. Peddemors. 2007. "A Computer-Aided Program for Pattern-Matching of Natural Marks on the Spotted Raggedtooth Shark *Carcharias taurus*." *Journal of Applied Ecology* 44, no. 2: 273–280. https://doi.org/10.1111/j.1365-2664.2006.01273.x.

Vyas-Patel, N., and J. D. Mumford. 2017. "I3S Classic and Insect Species Identification of Diptera and Hymenoptera (Mosquitoes and Bees)." *bioRxiv*. https://doi.org/10.1101/090621.

Walker-Milne, N. L., Y. P. Papastamatiou, S. D. Mahaffy, and R. W. Baird. 2025. "Dynamics of Foraging Interactions Between Cookiecutter Sharks (*Isistius* spp.) and Short-Finned Pilot Whales (*Globicephala macrorhynchus*) in Hawai'i." *Marine Biology* 172, no. 4: 1–12. https://doi.org/10.1007/s00227-025-04633-4.

Wang, J. 2016. "Individual Identification From Genetic Marker Data: Developments and Accuracy Comparisons of Methods." *Molecular Ecology Resources* 16, no. 1: 163–175. https://doi.org/10.1111/1755-0998.12452.

Wilson, B., P. S. Hammond, and P. M. Thompson. 1999. "Estimating Size and Assessing Trends in a Coastal Bottlenose Dolphin Population." *Ecological Applications* 9, no. 1: 288–300. https://doi.org/10.1890/1051-0761(1999)009[0288:ESAATI]2.0.CO;2.

Würsig, B., and T. A. Jefferson. 1990. "Methods of Photo-Identification for Small Cetaceans." In *Individual Recognition of Cetaceans: Use of Photo-Identification and Other Techniques to Estimate Population Parameters*. Report of the International Whaling Commission, Special Issue 12, edited by P. S. Hammond, S. A. Mizroch, and G. P. Donovan, 43–52. International Whaling Commission.

Yablokov, A. V., V. M. Bel'kovich, and V. I. Borisov. 1974. *Whales and Dolphins*. 520. Israel Program for Scientific Translations.

Zerbini, A. N., P. J. Clapham, and P. R. Wade. 2010. "Assessing Plausible Rates of Population Growth in Humpback Whales From Life-History Data." *Marine Biology* 157, no. 6: 1225–1236. https://doi.org/10.1007/s00227-010-1403-y.